Journal of Materials Chemistry B

Accepted Manuscript

ROYAL SOCIETY OF CHEMISTRY

www.rsc.org/materialsB

Table of contents

A novel magnetic polymer nanoparticle (Fe_3O_4@SiO_2@$(HA/CS)_{10}$-Ti^{4+} IMAC) was synthesized for the highly selective and effective enrichment of phosphopeptides.

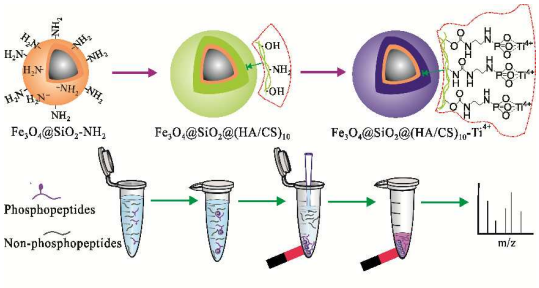

Journal of Materials Chemistry B

Cite this: DOI: 10.1039/c0xx00000x

www.rsc.org/MaterialsB

Paper

Ti^{4+}-immobilized multilayer polysaccharide coated magnetic nanoparticles for highly selective enrichment of phosphopeptides

Zhichao Xiong,[ab] Lingyi Zhang,[a] Chunli Fang,[b] Quanqing Zhang,[b] Yongsheng Ji,[bc] Zhang Zhang,[b] Weibing Zhang,[ab]* and Hanfa Zou[b]*

Received (in XXX, XXX) Xth XXXXXXXXX 20XX, Accepted Xth XXXXXXXXX 20XX
DOI: 10.1039/b000000x

Highly selective and efficient enrichment of trace phosphorylated proteins or peptides from complex biological sample is of profound significance toward the discovery of disease biomarkers in biological system. In this study, a novel immobilized metal affinity chromatography (IMAC) material was synthesized to improve the enrichment specificity and sensitivity for the phosphopeptides by introducing titanium phosphate moiety on multilayer polysaccharide (hyaluronate (HA) and chitosan (CS)) coated Fe_3O_4@SiO_2 nanoparticle (denoted as Fe_3O_4@SiO_2@$(HA/CS)_{10}$-Ti^{4+} IMAC). The thicker multilayer polysaccharide endows the excellent hydrophilic property and a higher capacity of titanium ion to the IMAC. Due to the combination of uniform magnetism property, highly hydrophilic property and enhanced binding capacity of titanium ion, the Fe_3O_4@SiO_2@$(HA/CS)_{10}$-Ti^{4+} nanoparticle possessed many merits, such as high selectivity for phosphopeptides (phosphopeptides/non-phosphopeptides at a molar ratio of 1:2000), extreme detection sensitivity (0.5 fmol), large binding capacity (100 mg g^{-1}), high enrichment recovery (85.45 %) and rapid magnetic separation (within 10 s). Moreover, the as-prepared IMAC nanoparticle display effective enrichment of phosphopeptide from the real samples (human serum and nonfat milk), showing great potential in detection and identification of low-abundance phosphopeptide as biomarker in biological sample.

Introduction

In recent years, extensive research has been carried out on the biomedical application of multifunctional nanomaterials.[1-5] Among these various nanomaterials, magnetic nanoparticles have been intensively investigated for their application in proteomic research due to their unique biocompatibility, easy preparation, controlled size, versatile modification and quick magnetic response.[6-8] As one of the most important and ubiquitous post-translational modifications, protein phosphorylation play vital roles in regulating many complex biological processes, such as cell division and growth, signaling transduction and metabolic pathways.[9, 10] Currently, mass spectrometry (MS) based techniques have been the premier technology for the characterization of the phosphorylation. However, the low abundance, low ionization efficiency, high complexity and severe ion suppression caused by the co-existence of abundance non-phosphopeptides make the MS directly analysis of phosphopeptides still a challenge. Thus, the selective enrichment of phosphoproteins/phosphopeptides from highly complicated mixture prior to MS analysis is indispensable.

To date, various materials and techniques including metal oxides affinity chromatography (MOAC),[11-14] immobilized metal ion affinity chromatography (IMAC),[15-19] strong cation exchange[20] and strong anion exchange[21] have been developed for the selective enrichment of phosphoproteins/phosphopeptides. Among them, IMAC is one of the most commonly used techniques,[22] in which the metal ions are immobilized on the polymer bead, porous bead and nanoparticle using linker molecule, and much efforts have been devoted to developing IMAC material. Traditionally, linkers such as iminodiacetic acid and nitrilotriacetic acid were used to chelate the metal ion.[23-25] However, the bound metal ions were easy to lose during the sample loading and washing procedure due to the relatively weaker interaction, which greatly reduced the enrichment efficiency. Recently, a new ligand of phosphate group was introduced to immobilized Ti^{4+} or Zr^{4+} ion to overcome the above drawback, and has been applied for phosphoproteome research.[26, 27] Nevertheless, most of the conventional IMAC material still require laborious separation procedure (*e.g.* centrifugation), which is not only inconvenient, but also may leads to undesirable nonspecificity peptides and loss of low-abundance phosphopeptides. Therefore, the design and synthesis of novel

IMAC material is still attracting attention to improve the phosphopeptides enrichment efficiency.

Combination of the magnetic nanomaterial with covalently bonding functional group could simultaneously achieve the simple and efficient separation of the target biomolecule from the complex mixture by using magnetic separation.[8] The functionalized magnetic nanoparticles have widely used in proteomic research including protein digestion,[28, 29] removal of abundance protein,[30] extraction of low-abundance peptide/protein,[31, 32] specific enrichment of glycopeptide and phosphopeptide,[33, 34] and capture of histidine-tagged peptide/protein.[35] In phosphopeptides enrichment, several kinds of IMAC magnetic nanoparticles (*e.g.* Fe_3O_4@SiO_2-Zr^{4+},[36] Fe_3O_4@C-Zr^{4+},[37] Fe_3O_4@mSiO_2-Zr^{4+},[38] and Fe_3O_4@PD-Ti^{4+} [39]) were developed and showed selectivity to capture phosphopeptides. However, the monolayer grafted and the relatively low density of the ligand on the surface for the immobilization of metal ion has limited the specificity, sensitivity and binding capacity for phosphopeptides. Therefore, it is highly desirable for an IMAC material with abundant ligand to achieve the immobilization of metal ion and to improve the selectivity and sensitivity for phosphopeptides.

Recently, the core-shell magnetic polymer nanoparticle with thick polymer shell, abundant functional group and good magnetic responsiveness make them become promising candidate for sample preparation in proteomic.[40-43] Ma et al. fabricated double polymer shells coated magnetic nanoparticles and anchored numerous Ti^{4+} ion with phosphate group and the material was utilized to selectively enrich phosphopeptides from complex biological sample.[42] Zhao et al. prepared PEG brushes grafted magnetic nanoparticles and immobilized abundant Ti^{4+} ion with reactive hydroxyl group.[43] The PEG brushes polymer enhanced binding amount of Ti^{4+} ion and binding capacity of phosphopeptides. Design and synthesis of novel polymer coating magnetic nanoparticles for improve the enrichment specificity and sensitivity to phosphopeptide is still breathtaking.

In this work, a novel IMAC material, Fe_3O_4@SiO_2@$(HA/CS)_{10}$-Ti^{4+} nanoparticle was designed and fabricated via a simple and reliable synthetic route (as shown in Scheme 1). The thicker polysaccharide polymer shell endow magnetic nanoparticle not only with excellent hydrophilic property, but also with numerous titanium phosphate moiety for large binding capacity and detection sensitivity of phosphopeptides. Moreover, the uniform magnetism property will facilitate the rapid and complete separation of IMAC nanoparticle. The performance of the IMAC nanoparticle in the phosphopeptides enrichment has been evaluated by using different biological samples. The high selectivity, excellent sensitivity, high enrichment recovery and large binding capacity of Fe_3O_4@SiO_2@$(HA/CS)_{10}$-Ti^{4+} nanoparticle for phosphopeptides clearly indicated the great potential as a high-performance IMAC material in phosphoproteome research.

Experimental section

Materials

Iron(III) chloride hexahydrate ($FeCl_3 \cdot 6H_2O$), ethylene glycol (EG), sodium acetate (NaAc), isopropanol and dimethyl sulfoxide (DMSO) were obtained from Tianjin Chemical Plant of chemical reagent (Tianjin, China). Tetraethyl orthosilicate (TEOS), 3-amine propyltrimethoxysilane (APTS), ammonia solution ($NH_3 \cdot H_2O$, 28-30 wt%), N-hydroxysuccinimide (NHS), 1-(3-dimethylaminoprophyl)-3-ethylcarbodiimide hydrochloride (EDC), chitosan (CS, low molecular weight), 1,1'-carbonyldiimidazole (CDI), 2,4,6-collidine, β-casein (from bovine milk), bovine serum albumin (BSA), trypsin (TPCK treated), dithiothreitol (DTT), iodoacetamide (IAA), urea, 2,5-dihydroxyl benzoic acid (DHB) and sodium bicarbonate ($NaHCO_3$) were purchased from sigma-Aldrich (St, Louis, MO, USA). Acetonitrile (ACN), trifluoroacetic acid (TFA) and formic acid (FA) were provided by Merck (Darmstadt, Germany). Sodium hyaluronate (HA) (Mw = 100 kDa) was obtained from Zhenjiang Dong Yuan Biotech Co., Ltd., (Zhenjiang, China). $Ti(SO_4)_2$ was purchased from Sinopharm. Chemical Reagents Co. Ltd (Shanghai, China). Human serum from healthy volunteer was provided by Dalian Medical University and stored at -80 □ before analysis. The nonfat milk was obtained from a local supermarket. Standard phosphopeptide (LRRApSLGGK) was from Shanghai Apeptide Co., Ltd., (Shanghai, China). Pure water (18.4 MΩ cm) used in all experiments was purified by a Milli-Q system (Millipore, Milford, MA, USA). All other chemicals were of analytical grade and used without purification.

Preparation of Fe_3O_4@SiO_2@$(HA/CS)_{10}$-Ti^{4+} magnetic nanoparticles

The Fe_3O_4 particles were prepared by a solvothermal reaction according to previous work.[24] 100 mg of Fe_3O_4 particles were dispersed in a mixture solution containing ethanol (200 mL), water (50 mL) and $NH_3 \cdot H_2O$ (1.5 mL) with 30 min sonication, then the mixture was stirred for 30 min at room temperature. TEOS (0.4 mL) was added into it and stirred for another 12 h. The resulted product was collected and successively washed with ethanol, water and isopropanol, then redispersed in isopropanol (30 mL). APTS (0.5 mL) was added dropwise and stirred for 24 h at room temperature. The obtained product (denoted as Fe_3O_4@SiO_2-NH_2) was separated using a magnet, washed three times with ethanol and dried at 50 □.

Fe_3O_4@SiO_2@$(HA/CS)_{10}$ nanoparticles were synthesized according to our previous work.[33] Typically, 50 mg of Fe_3O_4@SiO_2-NH_2 nanoparticles were activated with ethanol and dispersed in sodium hyaluronate solution (1 mg mL^{-1}, 0.135 mol L^{-1} NaCl, pH= 5), stirred for 20 min, and the product was collected by a magnet and washed three times with water to remove excess sodium hyaluronate. Then the nanoparticles were redispersed in chitosan solution (1 mg mL^{-1}, 0.135 mol L^{-1} NaCl, pH= 5) and stirred for 20 min, followed by magnetic separation and washing with water. After ten cycles, the product was collected, and immersed in PBS solution (10 mmol L^{-1}, pH= 5.5) containing EDC (2 mg mL^{-1}) and NHS (2 mg mL^{-1}). The mixture was stirred at room temperature overnight.

50 mg of Fe_3O_4@SiO_2@$(HA/CS)_{10}$ nanoparticles were dispersed in dried DMSO (10 mL), and CDI (500 mg) was added and the mixture was stirred for 24 h at room temperature. The resulted nanoparticles were collected and washed with DMSO, then redispersed in ethylenediamine (25 mL), stirred for 8 h at 60 □. The obtained product (denoted as Fe_3O_4@SiO_2@ $(HA/CS)_{10}$-

NH_2) was collected and washed three times with ACN. $Fe_3O_4@SiO_2@(HA/CS)_{10}$-$NH_2$ nanoparticles were dispersed in ACN solution (60 mL) containing $POCl_3$ (60 mmol L^{-1}) and 2,4,6-collidine (60 mmol L^{-1}), and the mixture was stirred at room temperature for 12 h under nitrogen atmosphere. After rinsed with ACN and water, the resulted nanoparticles (denoted as $Fe_3O_4@SiO_2@(HA/CS)_{10}$-$PO_4^{3-}$) were incubated in $Ti(SO_4)_2$ (60 mL, 50 mmol L^{-1}) aqueous solution at room temperature overnight under gentle stirring. The obtained nanoparticles (denoted as $Fe_3O_4@SiO_2@(HA/CS)_{10}$-$Ti^{4+}$) were collected and washed with CH_3COOH/H_2O (10:90, v/v, 200 mmol L^{-1} NaCl) and pure water six times to remove residual titanium ions, respectively. The obtained $Fe_3O_4@SiO_2@(HA/CS)_{10}$-$Ti^{4+}$ nanoparticles were dispersed in TFA/H_2O (0.1:99.9, v/v) before use.

Material characterization

Field emission scanning electron microscope (FE-SEM) image were collected at JSM-7001F scanning electron microscope and transmission electron microscopy (TEM) image was obtained by JEOL JEM-2000 EX transmission electron microscope (JEOL, Tokyo, Japan). Fourier-transformed infrared spectroscopy (FT-IR) characterization has been performed on Thermo Nicolet 380 spectrometer using KBr pellets (Nicolet, Wisconsin, USA). Thermogravimetric (TG) analysis was carried out under nitrogen atmosphere at a heating rate of 10 □ min^{-1} from 30 □ to 1000 □ (NETZSCH, Selb, Germany). The saturation magnetization curve was conducted on the Physical Property Measurement System 9T (Quantum Design, San Diego, USA) at room temperature. Inductively coupled plasma-atomic emission spectrometry (ICP-AES) was used to determine the amount of titanium ion immobilized on the nanoparticle (Schimadzu Scientific Instruments, Kyoto, Japan). Zeta (ζ) potential measurement was operated on Nano-ZS90 instrument in water at 25 □ (Malvern, Worcestershire, United Kingdom).

Tryptic digestion of standard protein

1 mg of β-casein was dissolved in NH_4HCO_3 (1 mL, 50 mmol L^{-1}, pH=8.3) and digested with trypsin (an enzyme/protein ratio of 1:40, w/w) at 37 ℃ for 16 h. BSA (2 mg) was denatured in urea (1 mL, 8 mol L^{-1}) and NH_4HCO_3 solution (50 mmol L^{-1}), after the addition of DTT (20 μL, 1 mol L^{-1}), the mixture was incubated at 56 ℃ for 1 h. Subsequently, IAA (7.4 mg) was added and incubated at room temperature in the dark for 45 min. The mixture was further diluted ten-fold with NH_4HCO_3 (50 mmol L^{-1}), and incubated with trypsin (an enzyme/protein ratio of 1:40, w/w) at 37 ℃ for 16 h.

Tryptic digestion of proteins extracted from nonfat milk

30 μL of nonfat milk was added into NH_4HCO_3 (1 mL, 25 mmol L^{-1}), and this solution was centrifugated at 16,000 rpm for 15 min. The supernatant was collected, then denaturation at 100 □ for 10 min. The supernatant was digested with trypsin (40 μg) at 37 ℃ for 16 h.

Selective enrichment of phosphopeptides

50 μg of $Fe_3O_4@SiO_2@(HA/CS)_{10}$-$Ti^{4+}$ nanoparticles were added into loading buffer (ACN/H_2O/TFA, 60:34:6, v/v/v, 400 μL) containing β-casein tryptic digest, BSA tryptic digest or proteins extracted from nonfat milk, and the mixture was gently incubated at room temperature for 20 min. After removing the supernate, the nanoparticles were washed three times with washing buffer 1 (ACN/H_2O/TFA, 60:34:6, v/v/v, 200 mmol L^{-1} NaCl) and washing buffer 2 (ACN/H_2O/TFA, 30:69.9:0.1, v/v/v), respectively. The captured phosphopeptides were eluted by $NH_3{\cdot}H_2O$ (2 × 10 μL, 10 wt%) by powerful shaking for 5 min. The eluate was directly analyzed by MALDI-TOF MS.

20 μL of human serum was diluted with pure water (120 μL) and denatured for 5 min in boiled water, then the diluted human serum (5 μL) was incubated with $Fe_3O_4@SiO_2@(HA/CS)_{10}$-$Ti^{4+}$ nanoparticles (100 μg) in loading buffer for 20 min. After discarding the supernate and washing with washing buffer 1 and washing buffer 2, the nanoparticles were eluted by $NH_3.H_2O$ (2 × 10 μL, 10 wt%), and the eluate was analyzed by MALDI-TOF MS.

Recovery test of phosphopeptide enrichment

A certain amount of standard phosphopeptide (LRRApSLGGK) was divided equally into two parts and labelled with light and heavy isotopes by using a stable isotope dimethyl labeling approach according to a previous reported procedure.[44] Then the heavy labelled phosphopeptide (1 pmol) was enriched with $Fe_3O_4@SiO_2@(HA/CS)_{10}$-$Ti^{4+}$ nanoparticles (50 μg) according to procedure mentioned above. The eluted section was mixed with the same amount of light labelled phosphopeptide (1 pmol), and the mixed peptides was analyzed by MALDI-TOF MS. The recovery of standard phosphopeptide was calculated by the MS intensity ratio of the heavy labelled phosphopeptide to the light labelled phosphopeptide.

Mass spectrometry analysis

All MALDI-TOF MS experiments were performed in reflector positive mode on AB Sciex 5800 MALDI-TOF/TOF mass spectrometer (AB Sciex, CA) with a pulsed Nd/YAG laser at 355 nm. Matrix DHB was dissolved in ACN/H_2O/H_3PO_4 (70: 29: 1, (v/v/v), 25 mg mL^{-1}). A 0.5 μL aliquot of the eluate and 0.5 μL of DHB matrix were sequentially dropped onto the MALDI plate for MS analysis.

Results and discusssion

The preparation procedure of $Fe_3O_4@SiO_2@(HA/CS)_{10}$-$Ti^{4+}$ nanoparticle with Fe_3O_4 as magnetic core, silica as intermediate layer, cross-linked polysaccharide as outer shell, and Ti^{4+} as immobilized affinity ion is illustrated in **Scheme 1**. Firstly, the Fe_3O_4 particle was synthesized by a solvethermal reaction, and coated with a silica layer via the sol-gel process, then reacted with APTES to get $Fe_3O_4@SiO_2$-NH_2 nanoparticle; Secondly, a thick and cross-linked polysaccharide layer was coated onto the nanoparticle via the layer-by-layer approach to form $Fe_3O_4@SiO_2@(HA/CS)_{10}$ nanoparticle; Thirdly, the terminal amine and hydroxyl groups on the polymer were converted into phosphate group by successively reacting with CDI, 1,2-enthanediamine and $POCl_3$; Finally, the titanium cations (Ti^{4+}) were immobilized onto the nanoparticle by the coordination reaction between Ti^{4+} and phosphate group to obtained the

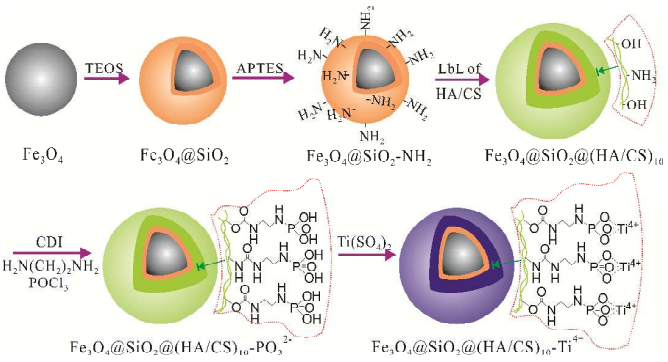

Scheme 1. Schematic illustration of the synthetic procedure for preparation of $Fe_3O_4@SiO_2@(HA/CS)_{10}$-$Ti^{4+}$ nanoparticle.

$Fe_3O_4@SiO_2@(HA/CS)_{10}$-$Ti^{4+}$ IMAC. For comparison, $Fe_3O_4@SiO_2$ nanoparticle without the polysaccharide shell was also modified with titanium phosphate (designated as $Fe_3O_4@SiO_2$-Ti^{4+}) according to the above procedure.

Characterization of $Fe_3O_4@SiO_2@(HA/CS)_{10}$-$Ti^{4+}$ magnetic nanoparticles

Representative TEM and FE-SEM images are shown in Fig. 1. The $Fe_3O_4@SiO_2$ nanoparticles (Fig. 1a) were comprised of a magnetic core (*ca.* 220 nm) and a thin layer of SiO_2 (*ca.* 3 nm). TEM image of $Fe_3O_4@SiO_2@(HA/CS)_{10}$ nanoparticles (Fig. 1b) clearly indicates that the cross-linked polysaccharide shell of hyaluronic acid and chitosan has been successfully coated on the surface of $Fe_3O_4@SiO_2$ nanoparticles, and the thickness of the polymer shell in the dry state is around 10 nm. After modifying the composite with phosphate group and Ti^{4+} ion, its structure and morphology has no significant change (Fig. 1c), indicating the

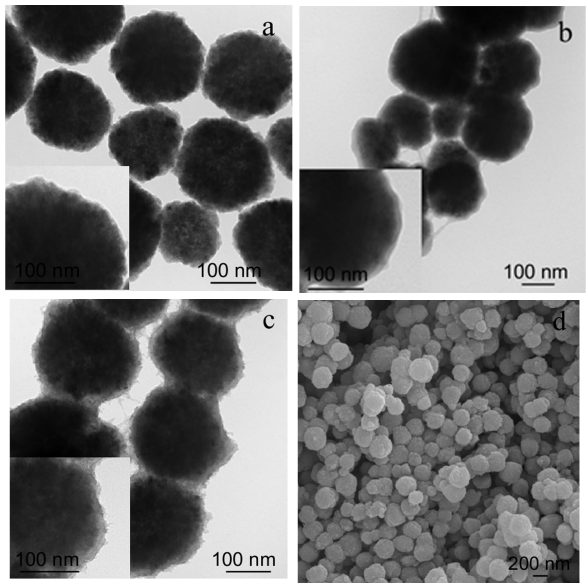

Fig. 1 TEM images of (a) $Fe_3O_4@SiO_2$, (b) $Fe_3O_4@SiO_2$ @$(HA/CS)_{10}$, (c) $Fe_3O_4@SiO_2@(HA/CS)_{10}$-$Ti^{4+}$, and FE-SEM image of (d) $Fe_3O_4@SiO_2@(HA/CS)_{10}$-$Ti^{4+}$ nanoparticles.

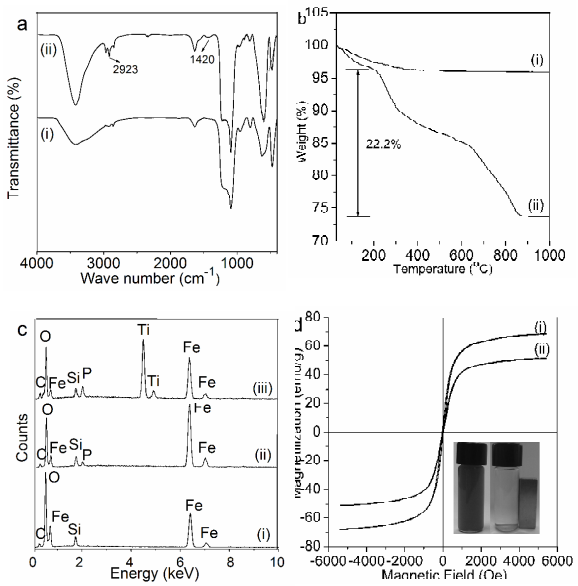

Fig. 2 (a) FT-IR spectra, (b) TG curves of (i) $Fe_3O_4@SiO_2$ and (ii) $Fe_3O_4@SiO_2@(HA/CS)_{10}$, (c) the EDX spectrum data of (i) $Fe_3O_4@SiO_2@(HA/CS)_{10}$, (ii) $Fe_3O_4@SiO_2@(HA/CS)_{10}$-$PO_3^{2-}$ and (iii) $Fe_3O_4@SiO_2@(HA/CS)_{10}$-$Ti^{4+}$, (d) magnetic hysteresis curves of (i) $Fe_3O_4@SiO_2$ and (ii) $Fe_3O_4@SiO_2@(HA/CS)_{10}$-$Ti^{4+}$ nanoparticles.

robust polymer shell structure. The FE-SEM image in Fig. 1d showing the $Fe_3O_4@SiO_2@(HA/CS)_{10}$-$Ti^{4+}$ nanoparticles have uniform shape and narrow size distribution.

FT-IR spectroscopy and thermogravimetric (TG) were used to inspect the cross-linked polysaccharide shell on $Fe_3O_4@SiO_2$ nanoparticle. Compared with the FI-IR spectrum of $Fe_3O_4@SiO_2$ (581 cm^{-1}, $\upsilon_{Fe\text{-}O\text{-}Fe}$, 1091 cm^{-1}, $\upsilon_{Si\text{-}O\text{-}Si}$), some new characteristic adsorption peaks (1420 cm^{-1}, $\upsilon_{C=O}$ of hyaluronic acid; 2923 cm^{-1}, $\delta_{C\text{-}H}$, $\upsilon_{C\text{-}H}$ of $-CH_3$) in the spectrum of $Fe_3O_4@SiO_2@(HA/CS)_{10}$ (Fig. 2a) could demonstrate the formation of the cross-linked polysaccharide shell. TGA curves indicated that the weight losses of 4.06 % of $Fe_3O_4@SiO_2$ attributed to the adsorbed water. It could be calculated that the weight loss of $Fe_3O_4@SiO_2@(HA/CS)_{10}$ was 22.2 % (Fig. 2b), which further demonstrated that the cross-linked polysaccharide polymer was successfully coated onto the nanoparticle.

Energy dispersive X-ray (EDX) spectra and zeta potential measurement were conducted to confirm the introduction of amine, phosphate group and titanium ion. As shown in Fig. 2c, the C, O, Fe, Si, P and Ti element peaks were found, indicating the successfully modification with phosphate group and titanium ion. In addition, the zeta potential values of four kinds of functionalized nanoparticles have also give the evidence for the successful immobilization of Ti^{4+} ion on $Fe_3O_4@SiO_2@(HA/CS)_{10}$ nanoparticle (Table S1, ESI †). The amount of immobilized Ti^{4+} on $Fe_3O_4@SiO_2@(HA/CS)_{10}$-$Ti^{4+}$ with a thick shell of cross-linked polysaccharide and $Fe_3O_4@SiO_2$-Ti^{4+} without the polymer shell measured ICP-AES are 44.38 μg mg^{-1} and 10.87 μg mg^{-1}, respectively, indicating the contribution of the high density of hydroxyl and amine groups on the cross-linked polysaccharide shell for the larger immolibilized amount of

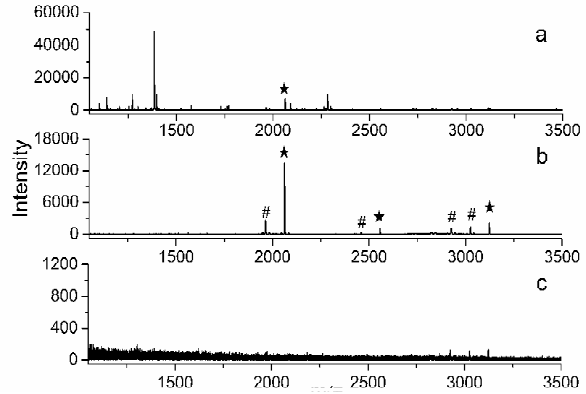

Fig. 3 MALDI-TOF mass spectra of the tryptic digest of β-casein (0.5 pmol). (a) direct analysis and after enrichment by (b) Fe_3O_4@SiO_2@$(HA/CS)_{10}$-Ti^{4+} and (c) Fe_3O_4@SiO_2@$(HA/CS)_{10}$ nanoparticles. ★ indicates phosphopeptides and # indicates dephosphorylated peptides.

titanium ion.

The magnetic properties of the two kinds of nanoparticles were studied using vibrating sample magnetometer at room temperature (Fig. 2d). The magnetic hysteresis loop curves show the two kinds of materials have no obvious remanence or coercivity at room temperature, suggesting that they all could be supermagnetic. As a comparison, the saturation magnetization (Ms) value of Fe_3O_4@SiO_2 nanoparticle was 68.08 emu g^{-1}. After coating the polymer layer and modification with phosphate group and titanium ion, the Ms value strikingly decreased to about 52.05 emu g^{-1}. A testing experiment showed that Fe_3O_4@SiO_2@$(HA/CS)_{10}$-Ti^{4+} nanoparticle can be easily dispersed in water in the absence of a magnetic field. Thanks to the high magnetic response of Fe_3O_4, the final product of Fe_3O_4@SiO_2@$(HA/CS)_{10}$-Ti^{4+} nanoparticle can also be easily rapid separated from the solution in only 10 s when a magnet was applied (insert in Fig. 2d).

Application in selective enrichment of phosphopeptides from tryptic digest of standard protein

To demonstrate the practicability of the Fe_3O_4@SiO_2@$(HA/CS)_{10}$-Ti^{4+} nanoparticle as IMAC stationary phase for the enrichment of phosphopeptides, a standard phosphoprotein (bovine β-casein) tryptic digest was used to evaluate its performance. β-casein tryptic digest was incubated with Fe_3O_4@SiO_2@$(HA/CS)_{10}$-Ti^{4+} in loading buffer, after isolating the nanoparticle from solution and washing with washing buffer, the captured phosphopeptides were eluted and deposited on the MALDI target for MALDI-TOF MS analysis. As shown in Fig. 3a, for the direct analysis of β-casein tryptic digest, only one phosphopeptide with weak MS signal intensity and low signal-to-noise (S/N) ratio was detected due to the low-concentration of phosphopeptides and severe signal suppression by the abundant non-phosphopeptides. However, after enrichment by Fe_3O_4@SiO_2@$(HA/CS)_{10}$-Ti^{4+}, three expected phosphopeptides (β_1, β_2 and β_3) could be clearly detected with strong MS signal intensities and S/N ratios, along with their dephosphorylated peptides (Fig. 3b), which were likely formed during the MALDI ionization process. The detail information of the captured

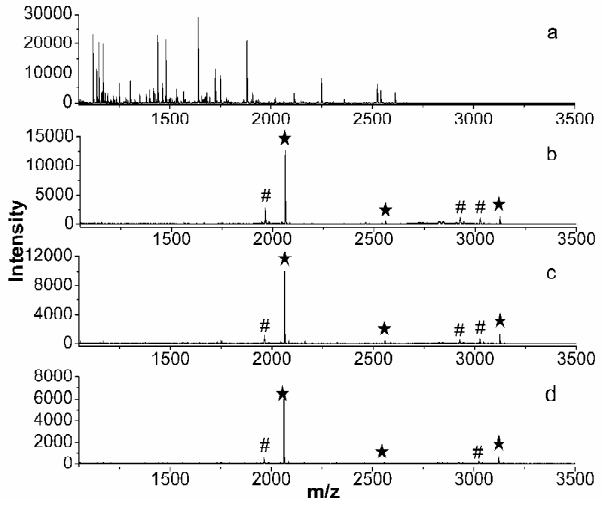

Fig. 4 MALDI-TOF mass spectra of the tryptic digest mixture of β-casein (0.5 pmol) and BSA. (a) direct analysis of peptides mixture at a molar ratio of 1:100; after enrichment by Fe_3O_4@SiO_2@$(HA/CS)_{10}$-Ti^{4+} nanoparticles at molar ratio of (b) 1:100, (c) 1:500, and (d) 1:2000. ★ indicates phosphopeptides and # indicates dephosphorylated peptides.

phosphopeptides from β-casein was displayed in Table S2 (ESI †). For comparison, the tryptic digest of β-casein was also treated with Fe_3O_4@SiO_2@$(HA/CS)_{10}$, no peak representing phosphopeptide was observed (Fig. 3c). These results demonstrated the enrichment selectively of Fe_3O_4@SiO_2@$(HA/CS)_{10}$-Ti^{4+} nanoparticle for phosphopeptides.

To evaluate the highly selectivity of the IMAC nanoparticle for the enrichment of phosphopeptides, a mixture of β-casein and BSA tryptic digest was used as the testing sample. As shown in Fig. 4a, when the molar ratio of β-casein and BSA was 1:100, no phosphopeptide was detected, while non-phosphopeptides peaks with high MS intensities were observed. However, after treatment by Fe_3O_4@SiO_2@$(HA/CS)_{10}$-Ti^{4+}, all the three phosphopeptides could be easily detected (Fig. 4b). Even when the molar ratio of β-casein and BSA was decreased to 1:500 and 1:2000, the three target phosphopeptides still can be distinctly identified with a clean background (Fig. 4c and Fig. 4d). These results indicated that the Fe_3O_4@SiO_2@$(HA/CS)_{10}$-Ti^{4+} nanoparticle have high selectivity for capture of phosphopeptides from a complex peptide mixture.

As the level of phosphopeptides in a complex biological sample could be much lower, the ability to enrich and detect phosphopeptides from highly diluted solution is a key parameter to evaluate the enrichment performance of the IMAC material. Therefore, β-casein tryptic digest with three low concentrations were treated with Fe_3O_4@SiO_2@$(HA/CS)_{10}$-Ti^{4+}, and the eluates were analyzed by MALDI-TOF MS. As shown in Fig. 5a, two phosphopeptides were clearly detected in 10 fmol of β-casein tryptic digest after enrichment. Even though the total amount of β-casein tryptic digest was decreased to as low as 0.5 fmol (Fig. 5c), one phosphopeptide could still be identified at S/N ratio of 19 with m/z of 2061.70. The resulted detection sensitivity was higher than many previous reported IMAC and MOAC

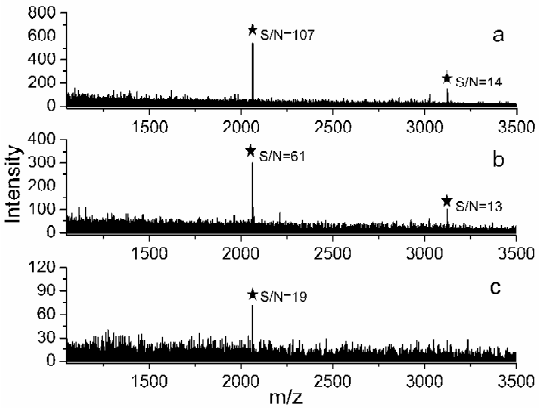

Fig. 5 MALDI-TOF mass spectra of tryptic digest of β-casein after enrichment by Fe_3O_4@SiO_2@$(HA/CS)_{10}$-Ti^{4+} nanoparticles. (a) 10 fmol (0.5 μL), (b) 2 fmol (0.5 μL) and (c) 0.5 fmol (0.5 μL). ★ indicates phosphopeptides.

nanomaterials such as Fe_3O_4@$mTiO_2$ (10 fmol),[12] Fe_3O_4@PD-Ti^{4+} (2 fmol),[39] Fe_3O_4@PMMA@PEGMP-Ti^{4+} (50 fmol),[42] mesoporous γ-Fe_2O_3 (50 fmol)[45] and Al_2O_3 hollow sphere (5 fmol).[46] The lower detection limit may attribute to the excellent hydrophilicity, large amount of immobilized Ti^{4+} ion and absolute magnetic separation of Fe_3O_4@SiO_2@$(HA/CS)_{10}$-Ti^{4+} nanoparticle. This result shows that the prepared Fe_3O_4@SiO_2@$(HA/CS)_{10}$-Ti^{4+} IMAC nanoparticle have high detection sensitivity for phosphopeptides.

To test the contribution of cross-linked polysaccharide shell on enrichment of phosphopeptides, the binding capacity of Fe_3O_4@SiO_2@$(HA/CS)_{10}$-Ti^{4+} and Fe_3O_4@SiO_2-Ti^{4+} were investigated, respectively. Different amount of nanoparticle was added to a fixed amount of β-casein tryptic digest (1 μg). After enrichment, the eluates (0.5 μL) were analyzed by MALDI-TOF MS. When the signal of one selected phosphopeptide (β_1) reached the maximum value, the total phosphopeptides were bonded onto the nanoparticle. As illustrated in Fig. 6a, the binding capacity of Fe_3O_4@SiO_2-Ti^{4+} nanoparticle was calculated to be about 40 mg g^{-1}, and the Fe_3O_4@SiO_2@$(HA/CS)_{10}$-Ti^{4+} nanoparticle showed binding capacity as high as 100 mg g^{-1}. The result indicated the cross-linked polysaccharide shell coated on the Fe_3O_4@SiO_2 has a significant effect on the immobilization capacity of titanium ion, resulting in larger binding capacity of phosphopeptides.

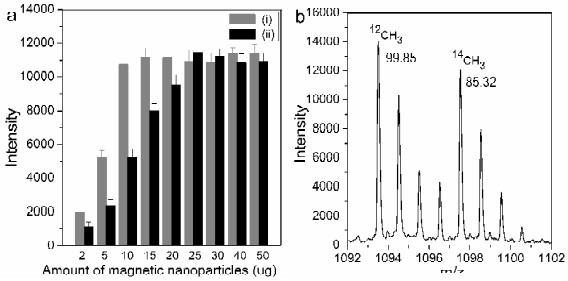

Fig. 6 (a) Comparison of phosphopeptides enrichment capacity between (i) Fe_3O_4@SiO_2@$(HA/CS)_{10}$-Ti^{4+} and (ii) Fe_3O_4@SiO_2-Ti^{4+} nanoparticles and (b) MALDI-TOF mass spectra of standard phosphopeptide LRRApSLGGK (a mixture of two $^{12}CH_3$-labeled unenriched and an equal amount of two $^{14}CH_3$-labeled enriched).

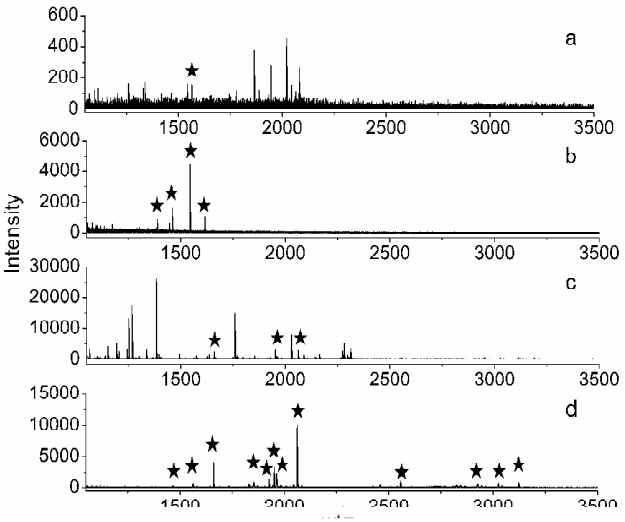

Fig. 7 MALDI-TOF mass spectra of human serum (a) before and (b) after enrichment by Fe_3O_4@SiO_2@$(HA/CS)_{10}$-Ti^{4+} nanoparticles. MALDI-TOF mass spectra of tryptic digests of the nonfat milk (c) before and (d) after enrichment by Fe_3O_4@SiO_2@$(HA/CS)_{10}$-Ti^{4+} nanoparticle. ★ indicates phosphopeptides.

The enrichment recovery of Fe_3O_4@SiO_2@$(HA/CS)_{10}$-Ti^{4+} nanoparticle for phosphopeptides was measured by using the quantitative approach of stable isotope dimethyl labelling. Two samples containing the same amount of standard phosphopeptide were labelled with light and heavy isotope, respectively.[44] The first part was treated with formaldehyde, and a 28 Da mass increase was produced by introducing two $^{12}CH_3$ at the N-termini of the lysine. The second part was reacted with deuterium formaldehyde, then two hydrogen atoms were replaced by two $^{14}CH_3$ and a 32 Da mass increase was produced. Then, the second part was treated with Fe_3O_4@SiO_2@$(HA/CS)_{10}$-Ti^{4+}, and the eluate was mixed with the first part and analyzed by MALDI-TOF MS. The MS intensity ratio of heavy to light labelled peptide reflects the recovery yield. As shown in Fig. 6b, the enrichment recovery of Fe_3O_4@SiO_2@$(HA/CS)_{10}$-Ti^{4+} for phosphopeptide was as high as 85.45 %. The result reveals the Fe_3O_4@SiO_2@$(HA/CS)_{10}$-Ti^{4+} nanoparticle could act as an ideal IMAC material for the enrichment of phosphopeptides.

Application in highly specific enrichment of phosphopeptides from human serum and nonfat milk

To further demonstrate the applicability of the Fe_3O_4@SiO_2@$(HA/CS)_{10}$-Ti^{4+} nanoparticle in selective enrichment of low-abundance phosphopeptides from practical biological sample, human serum and nonfat milk were applied as real samples. For diluted human serum, as shown in Fig. 7a, only one phosphopeptide with weak MS signal intensity appeared owing to the low-abundance phosphopeptides and high salt content. After treated with Fe_3O_4@SiO_2@$(HA/CS)_{10}$-Ti^{4+}, four peaks of phosphopeptides with higher MS intensities and a clean background can be clearly detected (Fig. 7b). The detailed information of the four phosphopeptides from human serum were given in Table S3 (ESI †). Similarly, the direct analysis result of the digested nonfat milk by MALDI-TOF MS was shown in Fig. 7c, only three weak MS signal intensities of phosphopeptides can

be detectable due to the interference of abundant non-phosphopeptides. However, eleven peaks of phosphopeptides were distinctly observed with a clean background after treatment with Fe_3O_4@SiO_2@$(HA/CS)_{10}$-Ti^{4+} (Fig. 7d). The detailed information of the eleven phosphopeptides from tryptic digest of proteins extracted from nonfat milk was given in Table S4 (ESI †). The results suggested that Fe_3O_4@SiO_2@$(HA/CS)_{10}$-Ti^{4+} nanoparticle is capable of highly selective trapping phosphopeptides from a naturally obtained complex biological sample.

Conclusions

To sum up, a novel IMAC nanomaterial, Fe_3O_4@SiO_2@$(HA/CS)_{10}$-Ti^{4+} nanoparticle, was successfully synthesized by introducing titanium phosphate moiety on cross-linked polysaccharide shell coated Fe_3O_4@SiO_2 nanoparticle for the enrichment of phosphopeptides with high specificity, extreme high detection sensitivity, large binding capacity and high enrichment recovery. The thick polysaccharide shell endows the nanoparticle not only excellent hydrophilic property, but also higher capacity of titanium ion, resulting in improving the selectivity and sensitivity for phosphopeptides. In the selective enrichment of phosphopeptides from human serum and drinking milk, the Fe_3O_4@SiO_2@$(HA/CS)_{10}$-Ti^{4+} nanoparticle show great practicability in identifying low-abundant phosphopeptides from complex biological samples. We believe that this work would help to design and prepare of more efficient and sensitive tool for phosphoproteome research.

Acknowledgements

Financial support is gratefully acknowledged from the National Natural Sciences Foundation of China (21235006), the Science and Technology Commission of Shanghai Municipality (12JG0500200), the Creative Research Group Project by NSFC (2132106), the National Key Scientific Instrument and Equipment Development Project (2012YQ120044), the China State Key Basic Research Program Grant (2013CB911202, 2012CB-910601 and 2012CB-910101), the Analytical Method Innovation Program of MOST (2012IM030900) and the Knowledge Innovation program of DICP to H. F. Zou.

Notes and references

[a] *Shanghai Key Laboratory of Functional Materials Chemistry, Department of Chemistry and Molecular Engineering, East China University of Science and Technology, Shanghai 200237, P.R. China. Fax: +86-021-64233161; Tel: +86-021-64252145 E-mail: weibingzhang@ecust.edu.cn*

[b] *Key Laboratory of Separation Sciences for Analytical Chemistry, National Chromatographic R&A Center, Dalian Institute of Chemical Physics, Chinese Academy of Sciences (CAS), Dalian 1160237, P.R. China. Fax: +86-0411-84379620; Tel: +86-0411-84379610 E-mail: hanfazou@dicp.ac.cn*

[c] *College of pharmacy, Henan University of Traditional Chinese Medicine, Zhengzhou 450000, China*

† Electronic supplementary information (ESI) available. See DOI: 10.1039/b000000x/

1 L. Y. Feng, L. Wu and X. G. Qu, *Adv. Mater.*, 2013, **25**, 168.

2 Y. J. Ma, R. J. Nolte and J. J. Cornelissen, *Adv. Drug Delive. Rev.*, 2012, **64**, 811.

3 C. Chung, Y. K. Kim, D. Shin, S. R. Ryoo, B. H. Hong and D. H. Min, *Acc. Chem. Res.*, 2013, **46**, 2211.

4 Y. L. Li, L. Zhu, Z. Z. Liu, R. Cheng, F. H. Meng, J. H. Cui, S. J. Ji and Z. Y. Zhong, *Angew. Chem. Int. Ed.*, 2009, **48**, 9914.

5 J. Khandare, M. Calderón, N. M. Dagia and R. Haag, *Chem. Soc. Rev.*, 2012, **41**, 2824.

6 J. Guo, W. L. Yang and C. C. Wang, *Adv. Mater.,* 2013, **25**, 5196.

7 X. S. Li, G. T. Zhu, Y. B. Luo, B. F. Yuan and Y. Q. Feng, *TrAC Trend. Anal. Chem.,* 2013, **45**, 233.

8 Y. Li, X. M. Zhang and C. H. Deng, *Chem. Soc. Rev.,* 2013, **42**, 8517.

9 J. Ptacek, G. Devgan, G. Michaud, H. Zhu, X. W. Zhu, J. Fasolo, H. Guo, G. Jona, A. Breitkreutz, R. Sopko, R. R. McCartney, M. C. Schmidt, N. R.ACHIDI, S. J. Lee, A. S. Mah, L. H. Meng, M. J. R. Stark, D. F. Stern, C. D. Virgilio, M. Tyers, B. Andrews, M. Gerstein, B. Schweitzer, P. F. Predki and M. Snyder, *Nature,* 2005, **438**, 679.

10 J. V. Olsen, B. Blagoev, F. Gnad, B. Macek, C. Kumar, P. Mortensen and M. Mann, *Cell,* 2006, **127**, 635.

11 Z. D. Lu, M. M. Ye, N. W. Li, W. W. Zhong and Y. D. Yin, *Angew. Chem. Int. Ed.,* 2010, **49**, 1862

12 W. F. Ma, Y. Zhang, L. L. Li, L. J. You, P. Zhang, Y. T. Zhang, J. M. Li, M. Yu, J. Guo, H. J. Lu and C. C. Wang, *ACS nano,* 2012, **6**, 3179.

13 G. Cheng, Y. L. Liu, Z. G. Wang, S. M. Li, J. L. Zhang and J. Z. Ni, *J. Mater. Chem. B*, 2013, **1**, 3661.

14 Q. H. Min, X. X. Zhang, H. Y. Zhang, F. Zhou and J. J. Zhu, *Chem. Commun.*, 2011, **47**, 11709.

15 T. S. Nühse, A. Stensballe, O. N. Jensen and S. C. Peck, *Mol. Cell. Proteomics*, 2003, **2**, 1234.

16 T. E. Thingholm, O. N. Jensen, P. J. Robinson and M. R. Larsen, *Mol. Cell. Proteomics,* 2008, **7**, 661-671.

17 J. Y.Ye, X. M. Zhang, C. Young, X. L. Zhao, Q. Hao, L. Cheng and O. N. Jensen, *J. Proteome Res.*, 2010, **9**, 3561.

18 H. J. Zhou, M. L. Ye, J. Dong, E. Corradini, A. Cristobal, A. J. Heck, H. F. Zou and S. Mohammed, *Nat. Protoc.*, 2013, **8**, 461.

19 F. Wang, Y. T. Zhang, P. Yang, S. Jin, M. Yu, J. Guo and C. C. Wang, *J. Mater. Chem. B*, 2014, **2**, 2575.

20 S. Mohammed and A. J. Heck, *Curr. Opin. Biotech.*, 2011, **22**, 9.

21 M. M. Dong, M. H. Wu, F. J. Wang, H. Q. Qin, G. H. Han, J. Dong, R. A. Wu, M. L. Ye, Z. Liu and H. F. Zou, *Anal. Chem.*, 2010, **82**, 2907.

22 T. E. Thingholm, O. N. Jensen and M. R. Larsen, *Proteomics*, 2009, **9**, 1451.

23 Y. H. Zhang, X. J. Yu, X. Y. Wang, W. Shan, P. Y. Yang and Y. Tang, *Chem. Commun.*, 2004, **40**, 2882.

24 X. Q. Xu, C. H. Deng, M. X. Gao, W. J. Yu, P. Y. Yang and X. M. Zhang, *Adv. Mater.*, 2006, **18**, 3289.

25 J. D. Dunn, E. A. Igrisan, A. M. Palumbo, G. E. Reid and M. L. Bruening, *Anal. Chem.,* 2008, **80**, 5727.

26 S. Feng, M. L. Ye, H. J. Zhou, X. G. Jiang, X. N. Jiang, H. F. Zou and B. L. Gong, *Mol. Cell. Proteomics*, 2007, **6**, 1656.

27 H. J. Zhou, M. L. Ye, J. Dong, G. H. Han, X. N. Jiang, R. A. Wu and H. F. Zou, *J. Proteome Res.*, 2008, **7**, 3957.

28 Y. H. Deng, C. H. Deng, D. W. Qi, C. Liu, J. Liu, X. M. Zhang and D. Y. Zhao, *Adv. Mater.*, 2009, **21**, 1377.

29 Y. Shen, W. Guo, L. Qi, J. Qiao, F. Y. Wang and L. Q. Mao, *J. Mater. Chem. B*, 2013, **1**, 2260.

30 J. L. Cao, X. H. Zhang, X. W. He, L. X. Chen and Y. K. Zhang, *J. Mater. Chem. B*, 2013, **1**, 3625.
31 Y. H. Deng, D. W. Qi, C. H. Deng, X. M. Zhang and D. Y. Zhao, *J. Am. Chem. Soc.*, 2008, **130**, 28.
32 W. D. Qu, H. M. Bao, L. Y. Zhang and G. Chen, *Chem. Eur. J.*, 2012, **18**, 15746.
33 Z. C. Xiong, H. Q. Qin, H. Wan, G. Huang, Z. Zhang, J. Dong, L. Y. Zhang, W. B. Zhang and H. F. Zou, *Chem. Commun.*, 2013, **49**, 9284.
34 Q. L. Deng, J. H. Wu, Y. Chen, Z. J. Zhang, Y. Wang, G. Z. Fang, S. Wang and Y. K. Zhang, *J. Mater. Chem. B*, 2014, **2**, 1048.
35 X. Y. Zou, K. Li, Y. Zhao, Y. B. Zhang, B. J. Li and C. P. Song, *J. Mater. Chem. B*, 2013, **1**, 5108.
36 L. Zhao, R. A. Wu, G. H. Han, H. J. Zhou, L. B. Ren, R. J. Tian and H. F. Zou, *J. Am. Soc. Mass Spectrom.*, 2008, **19**, 1176.
37 D. W. Qi, Y. Mao, J. Lu, C. H. Deng and X. M. Zhang, *J.Chromatog. A*, 2010, **1217**, 2606-2617.
38 J. Lu, Y. Li and C. H. Deng, *Nanoscale*, 2011, **3**, 1225-1233.
39 Y. H. Yan, Z. F. Zheng, C. H. Deng, X. M. Zhang and P. Y. Yang, *Chem. Commun.* 2013, **49**, 5055.
40 H. M. Chen, C. H. Deng and X. M. Zhang, *Angew. Chem. Int. Ed.*, 2010, **49**, 607.
41 Z. C. Xiong, L. Zhao, F. J. Wang, J. Zhu, H. Q. Qin, R. A. Wu, W. B. Zhang and H. F. Zou, *Chem. Commun.*, 2012, **48**, 8138.
42 W. F. Ma, Y. Zhang, L. L. Li, Y. T. Zhang, M. Yu, J. Guo, H. J. Lu and C. C. Wang, *Adv. Funct. Mater.*, 2013, **23**, 107.
43 L. Zhao, H. Q. Qin, Z. Hu, Y. Zhang, R. A. Wu and H. F. Zou, *Chem. Sci.*, 2012, **3**, 2828.
44 P. J. Boersema, R. Raijmakers, S. Lemeer, S. Mohammed and A. J. Heck, *Nat. Protoc.*,2009, **4**, 484.
45 Y. T. Zhang, L. Li, W. F. Ma, Y. Zhang, M. Yu, J. Guo, H. J. Lu and C. C. Wang, *ACS Appl. Mater. Interfaces*, 2013, **5**, 614.
46 J. Lu, S. Liu and C. H. Deng, *Chem. Commun.*, 2011, **47**, 5334.